Synthesis and biochemical evaluation of RNA containing an intrahelical disulfide crosslink

Charles R Allerson and Gregory L Verdine*

Department of Chemistry, Harvard University, Cambridge, MA 02138, USA

Background: Several factors impede the elucidation of RNA structure and function by X-ray and NMR methods, including the complexity of folded RNA motifs, the tendency of RNA to aggregate, and its ability to fold into multiple isomeric structures. The ability to constrain the process of RNA folding to give a single, homogeneous product would assist these investigations. We therefore set out to develop a synthetic procedure for the site-specific insertion of a disulfide crosslink into oligoribonucleotides. We also examined the ability of a crosslinked species to serve as a substrate for ricin, an RNA glycosylase.

Results: A convertible nucleoside derivative (C) suitable for the site-specific introduction of N^4-alkylcytidine residues into RNA has been developed. The corresponding C phosphoramidite was employed in the synthesis of an 8-mer oligonucleotide, 5'-CGGAGACG-3', which was then efficiently converted to an 8-mer containing two *S*-protected N^4-(2-thioethyl)C residues. Upon deprotection and air oxidation, the 8-mer efficiently formed an intramolecular disulfide bond, yielding a GAGA tetraloop presented on a two-base-pair CpG disulfide crosslinked ministem. We show that this ministem–loop is an excellent substrate for ricin. Control 8-mers lacking the disulfide crosslink were substantially poorer substrates for ricin.

Conclusions: The nucleoside chemistry described here should be generally useful for the site-specific introduction of a range of non-native functional groups into RNA. We have used this chemistry to constrain an RNA ministem through introduction of an intrahelical disulfide crosslink. That this tetraloop substrate linked to a two base-pair ministem is efficiently processed by ricin is clear evidence that ricin makes all of its energetically favorable contacts to the extreme end of the stem–loop structure, and that the two base pairs of the stem abutting the loop remain intact during recognition and processing by ricin.

Chemistry & Biology October 1995, **2**:667–675

Key Words: disulfide crosslink, ricin, RNA glycosylase, RNA modification, RNA structure

Introduction

RNA has numerous functions in addition to its role as a carrier of genetic information, including serving as a receptor for regulatory proteins [1,2], a substrate for processing enzymes [3–6] and a catalyst of chemical transformations [7–10]. Through *in vitro* evolution, RNA molecules have been selected for the ability to bind ligands [11–17] or to catalyze reactions [18–22]. Whether derived from natural or biochemical selection, RNA ligands and catalysts must attain a well defined three-dimensional fold in order to function properly. The determination of such folded structures at high resolution continues to present a formidable challenge, because of the unusual and characteristic properties of RNA as a biopolymer. The fact that there are regions in a folded RNA molecule in which the nucleosides are not base-paired predisposes RNA toward heterogeneous self-aggregation, especially at the high concentrations used in crystallization trials and NMR measurements. Unlike proteins, spontaneous folding of RNA sometimes produces mixtures of species that fail to coalesce to a single species upon equilibration. Even for those sequences that adopt a single, well defined fold, structure determination by high-resolution methods has proven difficult in comparison with proteins [23–29]. This situation has created the need for methods by which to constrain the three-dimensional structure of RNA [30–32], and thus force it to adopt a single folded structure. The ability to constrain and functionalize RNA structure also provides a powerful means to test alternative structural models for the active conformation of folded RNAs [33–35] and to gain information on RNA–protein interactions [36].

It has been shown that the structure of DNA can be constrained through the site-specific introduction of disulfide crosslinks [37,38]. This general strategy has led to the production of a variety of engineered DNA structures, including those containing locally stabilized and destabilized helices [37,39–41], frame-shifted base-pairs [40], induced bends [42], or stem–loops [43]. In naturally occurring tRNAs, disulfide crosslinks have been observed to form between neighboring 4-thiouridine residues [44]. Engineered crosslinks have been used to force RNA to form a stem–loop structure [45] and to provide independent validation for X-ray crystallographic structures of the hammerhead ribozyme [35]. In developing a strategy for site-specific crosslinking of RNA using disulfide chemistry we required that the chemistry for RNA modification should introduce a minimum of non-native functionality, permit placement at internal sites within duplex regions, allow ready variation of the length of the crosslink, and be fully compatible with solid-phase RNA synthesis. Here we report an approach that meets these criteria.

*Corresponding author.

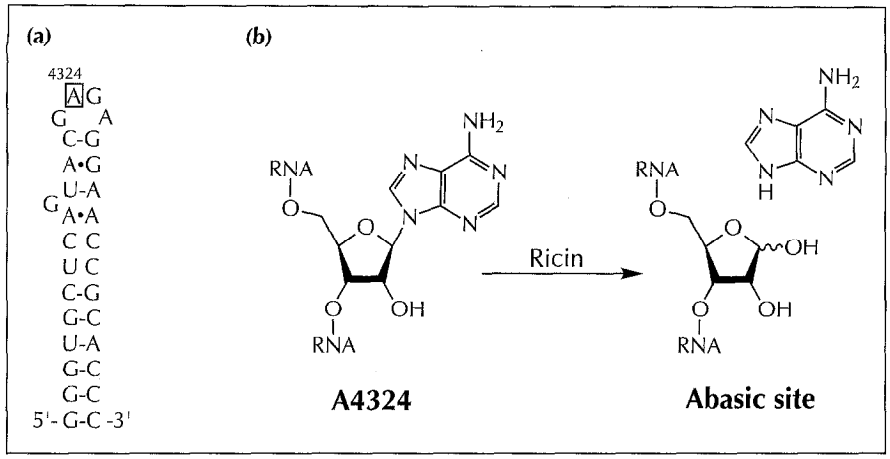

Fig. 1. Function of the ricin A-chain (RA). **(a)** Putative structure of 28S rRNA in the region targeted by RA. **(b)** RA catalyzes hydrolysis of the glycosidic bond of A4324 (indicated by the box in (a)).

To illustrate the application of this approach toward the study of RNA–enzyme interactions, we set out to engineer a minimal substrate for ricin, an RNA glycosylase [46]. Ricin, a member of a family of ribosome inhibiting proteins from plants [47], is so potently toxic that a single molecule is sufficient to kill a cell through inactivation of the eukaryotic ribosome; it therefore has potential use in chemical warfare. The enzyme is a heterodimer; one subunit (the A-chain) has catalytic activity, the other (the B-chain) mediates cellular import by binding to cell-surface carbohydrates. Upon internalization, the disulfide bond linking the two chains is reduced, and the free A-chain binds to the ribosome. The ricin A-chain (RA) binds to the eukaryotic 28S rRNA and catalyzes the hydrolysis of the N-glycosidic bond of the adenine residue at position 4324 (A4324, Fig. 1) [46,48]. This modification renders the ribosome inactive, possibly by preventing the recruitment of the eukaryotic elongation factor-2 to its recognition site [49]. RA is believed to recognize a stem–loop structure that places A4324 at the second position of a 5'-GAGA-3' loop [50]. This stem–loop is representative of a family of unusually stable RNA tetraloops having the consensus sequence 5'-GNRA-3' (N = any nucleotide, R = purine) [51]. NMR solution structures have been reported for several such tetraloops [52], including 5'-GAGA-3' [29,53,54]; these studies have indicated that, in the absence of associating proteins, the stem–loop adopts a compact structure in which the bases within the loop stack with neighboring bases of the stem. RA is relatively insensitive to the nucleotide composition of the stem, provided that base-pairing is maintained [55]. This result, together with the observation that RA can process a tetraloop substrate having a two base-pair stem (albeit only at a reduced temperature), suggests that the determinants of specific recognition lie principally if not exclusively within the tetraloop [50]. Little is known about the conformation of the tetraloop and attendant stem as it is bound by the enzyme. There is increased interest in this question following recent reports suggesting that DNA glycosylases [56,57], like DNA methyltransferases [58,59], substantially deform their duplex DNA substrates. Here we have examined the effect of tightly locking the RNA stem structure on recognition and catalysis by ricin.

Results

The synthesis described here extends earlier work in which we developed a general strategy for the post-synthetic attachment of functionalized tethers to specific sites in DNA [38,60]. In this procedure, a nucleoside derivative containing a leaving group, referred to as a 'convertible nucleoside', is incorporated into an oligomer during solid-phase synthesis. Treatment with an alkylamine results in the displacement of the leaving group and installation of an *N*-alkyl substituent in its place (Fig. 2). The amine used in the displacement step thus determines the structure of the tether. To apply this strategy to RNA modification, we synthesized the phosphoramidite of the convertible ribonucleoside 4-O-(4-chlorophenyl)uridine (Clϕ U) using standard procedures [60,61] (to be reported in detail elsewhere). The Clϕ U phosphoramidite was used in solid-phase synthesis of an 8-base oligoribonucleotide (8-mer) with the sequence 5'-(Clϕ U)GGAGA(Clϕ U)G-3'. In this synthesis, the Clϕ U phosphoramidite coupled with an efficiency equal to that of the G and A phosphoramidites. Treatment of the resin-bound 8-mer with 2 M methanolic cystamine resulted in conversion of the Clϕ U residue to an N^4-substituted C residue (Fig. 2). This treatment also resulted in the removal of the base- and phosphate-protecting groups from the RNA and in cleavage of the RNA from the solid support. The 2'-O-*tert*-butyldimethylsilyl (TBDMS) protecting groups were then removed by treatment with tetrabutylammonium fluoride (TBAF) to yield oligonucleotide **1a** (Fig. 3a). Parallel displacement reactions on the resin-bound 8-mer using either 7 M methanolic ammonia or 2 M methanolic 2-(methylthio)ethylamine, followed by TBAF deprotection, yielded an unmodified 8-mer (5'-CGGAGACG-3', WT8), or an 8-mer containing two N^4-2-(methylthio)ethyl-C moieties (MTE8), respectively. These controls were included to gauge the relative effects of crosslinking and tether attachment to the 8-mer on processing by RA. We also synthesized an unmodified 19-mer containing the GAGA tetraloop and a six-base-pair stem (5'-GGGCACUCAGAGAUGAGUG-3', WT19) to allow a direct comparison between our results and those of previous studies [50].

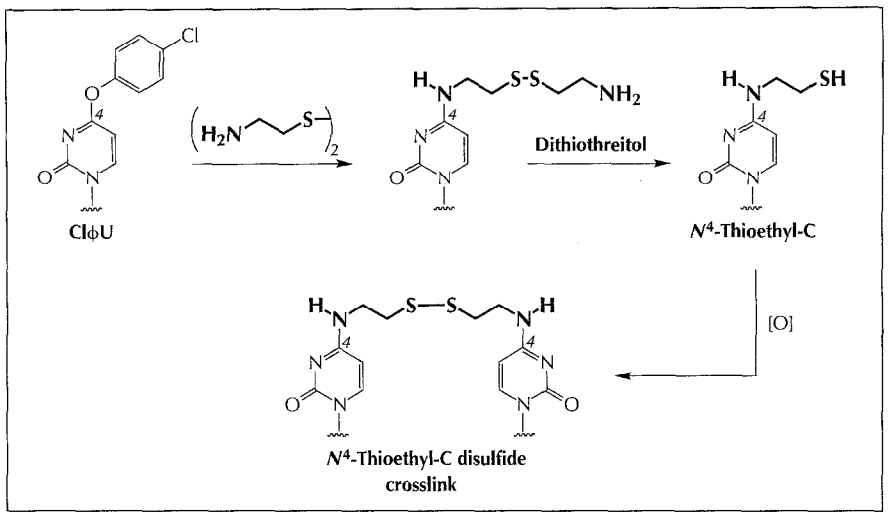

Fig. 2. Chemistry used in synthesis of disulfide crosslinked RNA. Displacement of the 4-chlorophenyl substituent from the convertible nucleoside ClϕU by cystamine gives an S-protected N^4-tethered-C residue, which upon reduction and oxidation forms the disulfide crosslink.

Treatment of compound **1a** with dithiothreitol (DTT) followed by ethanol precipitation and air oxidation gave a species having increased electrophoretic mobility in denaturing polyacrylamide gels (Fig. 3b, lane 4). Treatment of the oxidation product with DTT gave a different species having intermediate mobility. This behavior is consistent with a reaction scheme in which reduction of compound **1a** results in transient conversion to the bis-thiol **1b**, which rapidly oxidizes to produce XL8. Consistent with this scheme, reduction of XL8 generates a slower-migrating (i.e., less compact) species (Fig. 3b, lane 3), which is identical in mobility to the species produced by reduction of **1a** (Fig. 3b, lane 2). The common reduction product is assigned the structure **1b**. Further support for the assignment of the XL8 structure as the oxidation product was provided by nucleoside composition analysis, which revealed the presence of a disulfide-linked dimer of N^4-2-thioethyl-C (Fig. 4a). Nucleoside composition analysis of **1a** also revealed the presence of the corresponding mixed disulfide of N^4-2-thioethyl-C and cystamine (data not shown).

The apurinic site generated by the action of RA on its substrate undergoes degradation leading to strand scission upon treatment with aniline [62], whereas the starting RNA is unaffected by aniline. This forms the basis of a simple assay to detect the action of RA using the difference in electrophoretic mobility of the cleaved and uncleaved RNA. WT19, crosslinked 8-mer XL8, and control 8-mers WT8 and MTE8 were labeled at their 5' end with ^{32}P, exposed to RA under multiple turnover conditions, treated with aniline, and the products were separated by electrophoresis under denaturing conditions.

The assay conditions for multiple turnover were optimized (12:1 molar ratio of substrate:enzyme), and the RA-catalyzed deglycosylation of WT19 over time was compared to that of XL8 (Fig. 5). This analysis revealed that the enzyme processes the crosslinked ministem–loop at a rate similar to that observed with the substrate having a fully intact stem. Comparison of the entire panel of oligonucleotides in parallel RA-catalyzed cleavage reactions (Fig. 6) revealed that the native 8-mer WT8, is a poorer substrate than either WT19 or XL8; the tethered 8-mer control MTE8 is a substantially poorer substrate than even WT8.

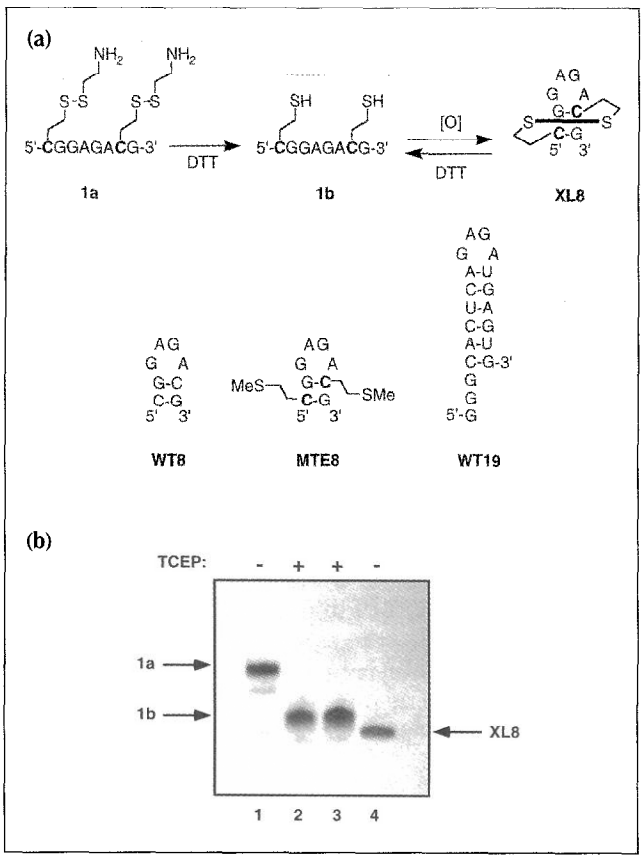

Fig. 3. Synthesis and characterization of a disulfide crosslinked ministem–loop. **(a)** Reduction of an 8-mer containing two S-protected N^4-thioethyl-C residues (**1a**) affords the corresponding dithiol (**1b**), which undergoes spontaneous air oxidation to form a ministem–loop structure (XL8). Other RNA molecules used in this study are represented below in the folded state. **(b)** Denaturing polyacrylamide gel electrophoresis showing that **1a** and XL8 produce a common intermediate upon reduction. The mobility of **1a** is retarded relative to **1b** because of the former's positively charged alkyl ammonium groups; XL8 possesses a more compact structure than **1b** and therefore migrates faster. TCEP = *tris*-(2-carboxyethyl)phosphine, a reducing agent used for reduction of disulfide bonds.

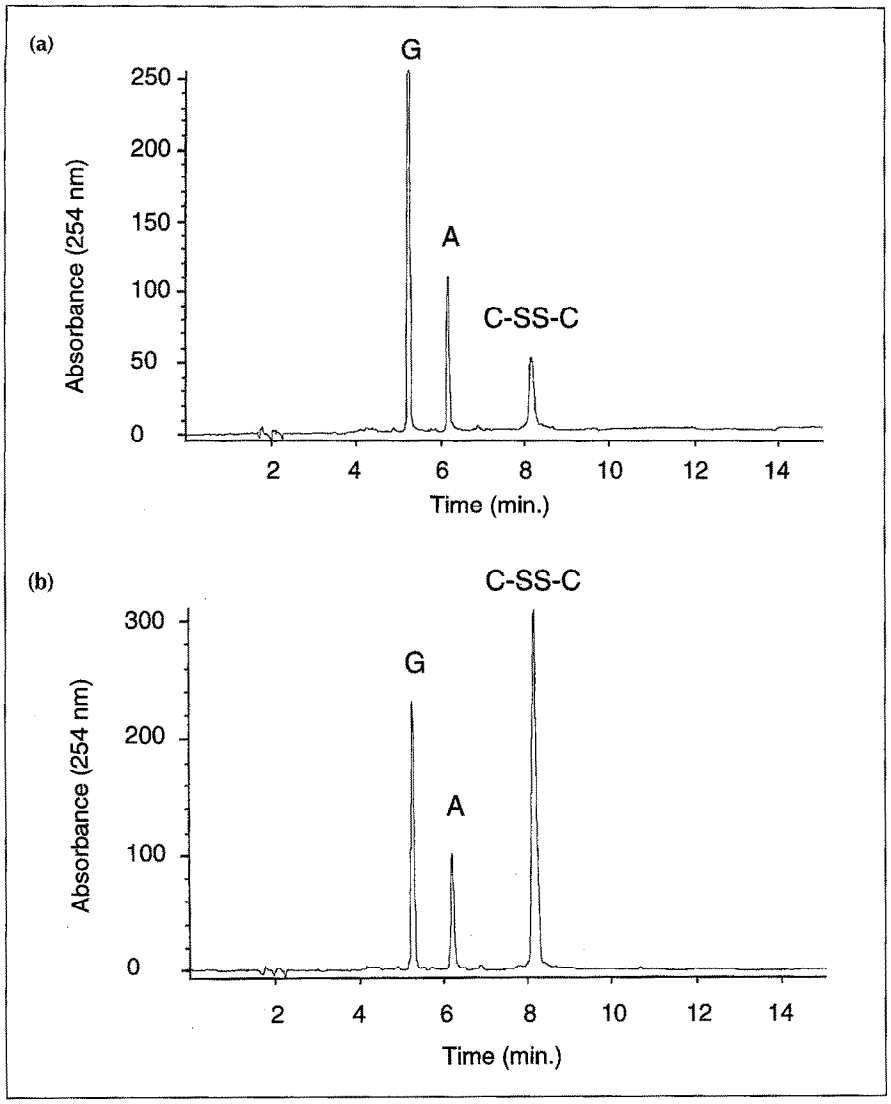

Fig. 4. Nucleoside composition analysis of XL8 confirms the presence of disulfide linked nucleosides. **(a)** Nucleoside products resulting from complete enzymatic digestion of XL8. The peak corresponding to the N^4-thioethyl-C disulfide is marked as C-SS-C. **(b)** Co-injection of the sample in (a) mixed with an authentic, synthetic standard of C-SS-C. Note the increase in the relative intensity of the C-SS-C peak in (b) as compared to (a).

To define more quantitatively the differences between the four substrates in recognition and cleavage by RA, we determined the Michaelis–Menten parameters k_{cat}, K_M and k_{cat}/K_M for each substrate. The results of this analysis are summarized in Table 1. Whereas the K_M value obtained for WT19 in our experiments is close to the reported value for this substrate (2.6 versus 5.7 μM, respectively), we observed a substantial increase in k_{cat} (0.71 versus 0.01 min^{-1}, respectively) [50], which presumably derives from the use of optimized assay conditions. The crosslinked substrate XL8 had very similar behavior to WT19, with a slight reduction in k_{cat} and increase in K_M giving rise to an overall 2.5-fold decrease in catalytic efficiency (k_{cat}/K_M). Surprisingly, the reduction in the rate of cleavage for WT8 was found to originate almost entirely from a substantial (10-fold) drop in k_{cat}. MTE8 suffers from significant deficiencies in both K_M and k_{cat}.

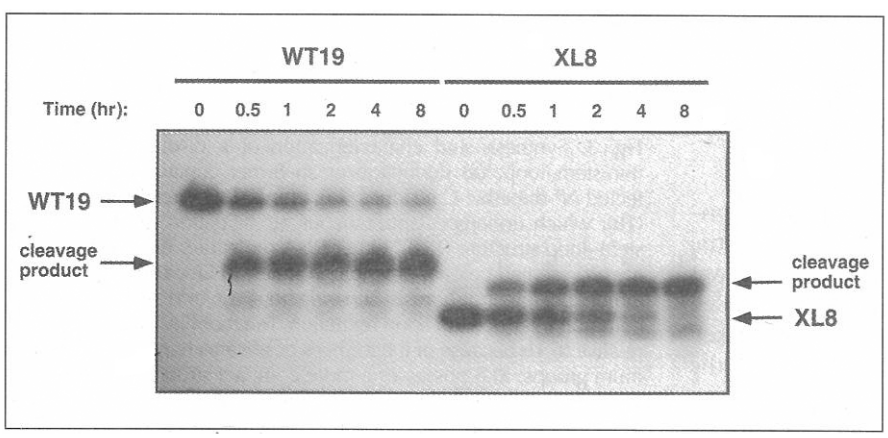

Fig. 5. RA processes the native 19-mer substrate WT19 and the disulfide crosslinked 8-mer XL8 at similar rates. RNA concentration, 6 μM; RA concentration 0.5 μM. In the case of WT19, RA processing followed by aniline cleavage generates a radiolabeled product that is smaller (10-mer) than the starting RNA. However, in the case of XL8, the two cleavage products remain linked together by the disulfide bond, and hence migrate slower (less compact structure) than XL8. Reduction of the RA/aniline-cleavage product of XL8 by TCEP yields a band having faster mobility than XL8 (data not shown).

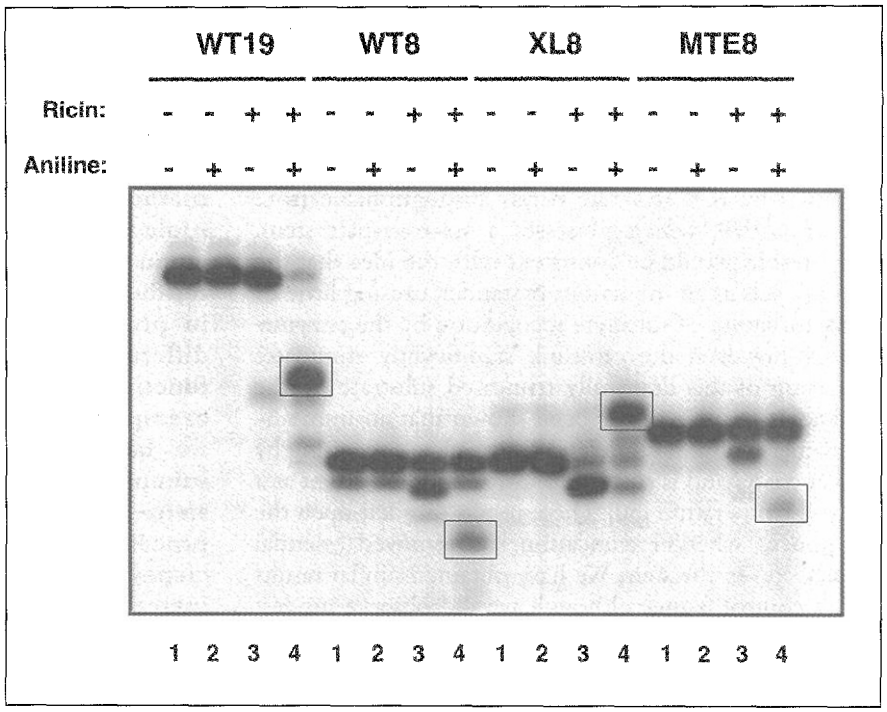

Fig. 6. Comparison of the efficiency of RA processing of native, crosslinked, and tethered oligonucleotides. In all of the oligonucleotides, a small fraction (~10 %) could not be cleaved. Correcting for this background, cleavage has proceeded to the following extents in this experiment: WT19, >98 %; WT8, 26 %; XL8, 85 %; MTE8, 13 %. The products of RA/aniline cleavage of each oligonucleotide are boxed.

Discussion

Here we have demonstrated an operationally simple method for attaching tethered functional groups to cytidine residues in RNA. The position of attachment, namely the exocyclic amino groups of the heterocyclic base, is fully compatible with duplex RNA structure, since the tether projects out from the floor of the major groove, with no disruption of Watson–Crick base-pairing functionality. The disulfide crosslinked CpG sequence can therefore be incorporated even into internal positions of a duplex segment of RNA without disturbing the helical structure. This feature should be especially useful in testing for the presence of coaxially stacked helices in complex RNA species such as the *Tetrahymena* self-splicing intron [33] or the products of SELEX (systematic evolution of ligands by exponential enrichment) procedures [11]. The method reported here thus offers an advantage over an alternative one that is incompatible with internal positions in duplex RNA [45]. The presence of the tether is also unlikely to interfere with other, non-standard pairing configurations commonly found in RNA, except for the possible case in which both protons of the exocyclic amine donate hydrogen bonds. In such cases, one could turn to the complementary approach of Eckstein and co-workers [35], in which the thiol-bearing tether is attached to the 2'-position of the sugar moiety.

The method reported here involves the use of convertible nucleoside chemistry to incorporate alkanethiols into DNA site-specifically for the purpose of generating defined crosslinks. The convertible nucleoside chemistry permits a broad range of functionalized tethers to be installed site-specifically into RNA (C.R.A. and G.L.V., unpublished results), because alkylamines bearing a wide variety of functional groups will react with the Clϕ U moiety. Recently, for example, pre-mRNA splicing substrates containing a single N^6-alkylamino-A residue were specifically functionalized with a photoaffinity label, allowing the temporal dynamics of protein association within the spliceosome to be followed [36]. This example also demonstrates the power of the convertible nucleoside approach toward site-specific RNA modification when used in conjunction with methods for fragment assembly of large RNA molecules through splinted ligation [63]. In work soon to be reported, we have also extended the convertible nucleoside approach to permit tethering to the exocyclic amino groups of A and G residues in the major and minor grooves, respectively (C.R.A., S.L. Chen and G.L.V., unpublished results).

Table 1. Michaelis–Menten kinetic parameters for RA processing of RNA substrates.

Substrate	k_{cat} (min^{-1})	K_M (μM)	k_{cat}/K_M (min^{-1} μM^{-1})
WT19	0.71 ± 0.22	2.6 ± 1.9	0.27 ± 0.12
XL8	0.41 ± 0.09	3.9 ± 2.6	0.11 ± 0.03
WT8	0.039 ± 0.010	4.6 ± 1.4	0.0085 ± 0.007
MTE8	0.026 ± 0.005	11.3 ± 2.0	0.0023 ± 0.002

We chose ricin for the initial exploration of this disulfide crosslinking approach because the interaction of RNA with this protein is well understood biochemically, and such a catalytic system is expected to impose a stringent test for structural perturbations caused by the crosslink. It is remarkable that the crosslinked 8-mer XL8 is processed by RA at a rate barely distinguishable from that of WT19, which possesses a six-base-pair stem. These results would be consistent with the idea that the crosslink acts as an innocuous bystander, causing little or no perturbation of substrate recognition by the enzyme. In fact, however, the crosslink significantly stimulates processing of this drastically truncated substrate by the enzyme. It has previously been shown that an unmodified 8-mer is almost completely resistant to processing by ricin at 37 °C and is cleaved to only a modest extent at a reduced temperature [50]. These results thus left open the question of whether truncation had removed essential contact sites in the stem. We have obtained similar results with a control 8-mer, although we did observe modest cleavage even at 37 °C. Only through crosslinking has it now been possible to obtain definitive evidence that ricin does not make energetically valuable contacts beyond the first two nucleotides of the stem. If RA does make direct contact with the first two base-pairs of the stem, these contacts almost certainly involve the sugar-phosphate backbone and not the bases themselves, as the enzyme tolerates changes in the sequence of the stem, provided that base-pairing ability is maintained [50]. We caution, however, that neither of these minimal substrates are as efficiently recognized and processed as the eukaryotic ribosome, for which RA has a k_{cat}/K_M of 683 min^{-1} μM^{-1} [48]. Thus, it seems likely that RA makes additional contacts outside the substrate stem–loop, perhaps even to protein components of the ribosome, that improve its catalytic efficiency.

Comparison of the kinetic parameters for RA cleavage of crosslinked and non-crosslinked oligonucleotides yielded unexpected results. If RA indeed recognizes a stem–loop structure and the crosslink itself is innocuous to the enzyme, one would expect the K_M of the crosslinked 8-mer to be lower than that of the unmodified 8-mer control, because crosslinking should stabilize the obligate stem–loop structure. On the other hand, assuming simplistically that k_{cat} reflects an event involving covalent bond-making or -breaking within a preformed Michaelis complex, then one would expect the k_{cat} for the two 8-mers to be very similar. The data reveal just the opposite, however; the most significant difference between the crosslinked and unmodified 8-mer is observed in k_{cat} rather than K_M. The origins of these effects are unclear. The higher K_M of MTE8 as compared with WT8 presumably reflects the energetic cost of forming the disfavored *anti* rotamer about the C^4-N^4 bond, as is required for Watson–Crick base-pairing [64]. Finally, the low K_M and high k_{cat} values observed for the crosslinked 8-mer, in which separation of the base-pair is essentially precluded, provide direct evidence that these base-pairs remain intact throughout the entire enzymatic processing reaction.

Significance

Enforcing a particular configuration on RNA should increase conformational homogeneity and decrease heterogenous self-aggregation, thus facilitating structural studies. Here we present a method for locking the segments of an RNA molecule together through disulfide crosslinks emanating from the exocyclic amine of C residues. This procedure should be useful not only in producing predefined structures, but also in differentiating between alternative models for the functional form of a folded RNA molecule. To exemplify the utility of disulfide crosslinked RNA, we have analyzed the ability of the catalytic subunit of ricin to process an 8-nucleotide mini-stem–loop. It is remarkable that the enzyme processes this minimal substrate with an efficiency approaching that of a 19-mer that has an intact stem. We thus conclude that the principal determinants of ricin A-chain recognition of its processing site lie within the tetraloop and first two nucleotides of the stem. This information may be of use in designing small molecules that will counter the severe cytotoxic effects of ricin, a potential chemical warfare agent.

Materials and methods

All glassware was pretreated with 1 % (v/v) diethylpyrocarbonate in ethanol, and all solutions and buffers were autoclaved to 120 °C for at least 30 min. UV spectra and absorbances were collected with an HP 8452 UV-vis spectrophotometer with a photodiode array detector. HPLC analyses were carried out on an HP 1090 Liquid Chromatograph equipped with a Beckman C18 reversed-phase column, using a gradient of acetonitrile in 0.1 M triethylammonium acetate (TEAA). A FUJIX BAS 2000 phosphorimager was used in the quantification of end-labeled RNA following gel electrophoresis. N-PAC phosphoramidites and solid phase supports (CPG) were obtained from Biogenex (San Ramon, CA). RNA syntheses were performed using an ABI 392 DNA/RNA synthesizer equipped with a conductance trityl monitor, using a modified version of the 1 μM RNA synthesis program and an extended coupling time of 15 min. Ricin A-chain was obtained from ICN Biomedicals, Inc. (Costa Mesa, CA), and all other enzymes were from Pharmacia (Piscataway, NJ). All chemicals were obtained from Aldrich Chemical, Inc. (Milwaukee, WI), with the exception of 2-(methylthio)ethylamine, which was purchased from Fluka (Ronkonkoma, NY).

Oligonucleotide synthesis and deprotection

All phosphoramidites, including the Clϕ U phosphoramidite, were dissolved to a concentration of 0.1 M in anhydrous CH_3CN. All syntheses proceeded with average stepwise yields of greater than 97 %. The resin-bound oligonucleotide, 5'-GGGCACUCAGAGAUGAGUG-3' (WT19) was treated with 1.5 ml of methanolic ammonia solution (7 M, saturated at 0 °C), at room temperature for 14 h [65]. The resulting solution was concentrated under vacuum using a Speed-Vac Concentrator (Savant). The resin-bound 8-mer containing the Clϕ U convertible nucleoside (5'-(Clϕ U)GGAGA(Clϕ U)G-3') was cleaved, deprotected, and converted to each of the three

2'-O-TBDMS-protected 8-mers in a single step. For the preparation of WT8, 1 μmol of the CPG-bound oligonucleotide was treated with methanolic ammonia and worked up as with WT19. To prepare MTE8, a 1 μmol portion of the CPG-bound convertible oligonucleotide was treated with 400 μl of a 2 M solution of 2-(methylthio)ethylamine in methanol for 18 h at 42 °C. To prepare the cystamine mixed-disulfide **1a**, a 1 μmol portion of CPG was treated with 400 μl of 2M cystamine (in methanol) for 18 h at 42 °C. Both the cystamine and 2-(methylthio)ethyl reactions were neutralized with acetic acid, and lyophilized.

Removal of the 2'-O-silyl ethers was afforded by treating each of the oligonucleotides with 0.6 ml of 1M tetrabutylammonium fluoride in THF for 20 h at room temperature. These reactions were quenched by the addition of 0.75 ml of 1M TEAA, pH 7.5. The oligonucleotides were then desalted by loading onto a C18 SepPak cartridge (Waters/Millipore), followed by elution with 30 % CH_3CN/0.1 M triethylammonium bicarbonate and lyophilization to a solid.

Oligonucleotide purification

The crude deprotected oligonucleotides were purified using denaturing polyacrylamide gel electrophoresis. All gels were 20 % polyacrylamide (19:1 acrylamide/bis-acrylamide) using a TBE running buffer (90 mM Tris free base, 90 mM boric acid, and 2 mM Na_2EDTA, pH 8.3). The product oligonucleotides were visualized on the gel by UV-shadowing over a fluorescent-active TLC plate, excised from the gel, crushed, then soaked overnight at 37 °C with 10 ml of 1M ammonium acetate. The resulting solution was desalted on a C18 SepPak cartridge to afford purified RNA oligomer as a dry, off-white solid. Oligonucleotides were quantified by UV absorbance at 260 nm, assuming an extinction coefficient of 1.0 x 10^4 M^{-1} cm^{-1} per nucleotide.

Crosslinking of XL8

The mixed-disulfide-containing oligonucleotide **1a** (220 nmol) was dissolved in 150 μl of deionized, distilled H_2O (ddH_2O), to which 150 μl of 60 mM dithiothreitol (DTT) was added. This solution was vortexed then heated to 55 °C for 2 h. Addition of 0.3 ml of 3 M NaOAc was followed by ethanol precipitation. The resulting RNA pellet was dissolved in 20 ml of 25 mM ammonium acetate for a final concentration of ~10 μM in oligonucleotide. This solution was allowed to air-oxidize for 20 h at room temperature, then concentrated on a Speed-Vac concentrator and purified by 20 % denaturing polyacrylamide gel electrophoresis (PAGE), as described above. The crosslinked oligonucleotide was visualized by UV-shadowing (appearing as the only major band), and isolated as described, yielding 146 nmol (66 % yield from the initial 220 nmol of **1a**) of pure XL8 as quantified by UV absorbance at 260 nm. After PAGE purification, all oligonucleotides were dialyzed against 3l of 10 mM NaCl, 5 mM TrisHCl (pH 7.5) for 36 h using 500 MWCO Spectra/Por CE (cellulose-ester) dialysis tubing from Spectrum Medical Industries, Inc. (Houston, TX), to remove any contaminants from gel purification (particularly ammonium ion).

Enzymatic digestion analysis

In a typical digestion analysis, 8 nmol of oligonucleotide was dissolved in 60 μl of a solution containing 0.2 mM $ZnCl_2$, 16 mM $MgCl_2$, 250 mM Tris-HCl (pH 6.0), 0.2 units of snake venom phosphodiesterase (Pharmacia) and 4 units of calf intestinal alkaline phosphatase (Boehringer Mannheim), and was heated at 37 °C for 8 h. Samples were then injected onto a reversed-phase C18 HPLC column (Waters/Millipore) with a gradient elution from 100 % 0.1 M TEAA to 50 % acetonitrile/50 % 0.1 M TEAA over 15 min (flow rate 1.5 ml min^{-1}). The identity of modified nucleosides was verified by coinjection with authentic nucleoside standards; nucleoside identity was also confirmed using photodiode array UV spectra. The authentic nucleoside standards of N^4-(methylthioethyl)-cytidine, N^4-thioethyl-C/cystamine mixed disulfide, and N^4-thioethyl-cytidine disulfide were prepared separately and were characterized by ^1H NMR and fast-atom bombardment high-resolution mass spectrometry (FAB-HRMS).

Electrophoretic analysis of crosslink formation

To compare the reduction product of compound **1** with the reduction product of XL8 (Fig. 3b), 1.5 nmol of both compound **1** and XL8 were treated with 5 μl of 20 mM *tris*-(2-carboxyethyl)phosphine (TCEP) in 50 mM TrisHCl, pH 7. The resulting solutions were heated to 80 °C for 15 min, and were immediately loaded onto a 20 % denaturing gel. After electrophoresis for 4 h at 350 V, the gel was stained with methylene blue (Fig. 3b).

5'-^{32}P Endlabeling of oligonucleotides

RNA was 5'-^{32}P-endlabeled using a standard procedure. Generally, 10 pmol of oligonucleotide was prepared in a solution of Pharmacia One-Phor All Plus buffer (50 mM KOAc, 10 mM Tris-acetate, 10 mM $Mg(OAc)_2$), 5 units of T4 polynucleotide kinase (Pharmacia), and 40 μCi of γ-^{32}P ATP (DuPont-NEN) and was heated to 37 °C for 2 h, quenched by the addition of 0.3 M Na_2EDTA, then extracted with 25:24:1 phenol/chloroform/isoamyl alcohol (2 x 150 μl). Addition of 50 μl 3M NaOAc was followed by ethanol precipitation using 20 μg of glycogen as a coprecipitant.

Optimization of RA reaction conditions

In initial attempts to evaluate the processing of the four substrates by RA, we noted unacceptably high levels of variability in the efficiency of the enzymatic reaction. This prompted us to examine the effect of various additives on the activity of RA. It was previously reported that RA is inhibited by monovalent cations, particularly Na^+, K^+, and NH_4^+ [48]. We also detected suppression of RA activity by Na^+, at concentrations far lower than previously observed. Significant reduction in enzyme activity was observed at 20 mM NaCl, with processing being almost fully inhibited at 100 mM. We detected inhibition by NH_4^+ at >20 mM, but none by KCl up to 30 mM. The presence of bovine serum albumin also led to a substantial decrease in RA activity. EDTA was found to be absolutely essential for enzymatic activity, and the addition of glycerol to 11 % also greatly improved the efficiency of RA (data not shown).

Reactions with RA

Ricin A-chain (RA) was prepared as a 40 μM RA stock solution in 10 mM TrisHCl (pH 7), 50 mM KCl, and 40 % glycerol. RA is stable for at least 6 months in this solution when stored at 4 °C. Solutions of each oligonucleotide were prepared to be 10 mM TrisHCl (pH 7), 20 mM KCl, 10 mM $MgCl_2$, 8–12.5 μM unlabeled RNA and 50 nM ^{32}P-endlabeled RNA [50]. These solutions were self-annealed by heating to 95 °C for several minutes, then cooling to room temperature over 2 h.

To compare the relative reaction rates for WT19 and XL8, reaction solutions were made to a volume of 50 μl containing 6 μM RNA, 0.5 μM RA, 3 mM Na_2EDTA, 10 mM KCl,

5 mM TrisHCl, 4 mM $MgCl_2$ and 11 % glycerol. Samples were incubated at 37 °C. Aliquots of 5 μl were removed and quenched at 0.5, 1, 2, 4 and 8 h.

To compare relative reactivities of the four oligonucleotides in Figure 6, reaction solutions were prepared to contain 4 μM RNA, 3 mM Na_2EDTA, 10 mM KCl, 5 mM TrisHCl, 4 mM $MgCl_2$, 11 % glycerol, and 0.5 μM RA to a final volume of 50 μl. The reaction solutions were incubated at 37 °C for 5 h.

Determination of kinetic parameters

In the determination of initial reaction velocities at 37 °C, each reaction was made up to a volume of 20 μl in 10 mM KCl, 5 mM TrisHCl, 4 mM $MgCl_2$, 2 mM Na_2EDTA and 11 % glycerol, with RNA concentrations ranging from 1.0 μM to 10.0 μM. Optimization of experimental conditions resulted in slightly different RA concentrations and incubation times for each of the four substrates. For WT19, the RA concentration was 25 nM, and reactions were incubated for 10 min. For XL8, the RA concentration was 0.1 μM and the reactions were incubated for 10 min. For both WT8 and MTE8, the RA concentration was 0.5 μM, and reaction times were 20 min and 45 min, respectively. Following gel electrophoresis and radioactive quantitation, double-reciprocal (Lineweaver–Burke) plots were generated and values of k_{cat} and K_M were calculated.

All reactions with RA were quenched by the addition of 10 μl of 1 % sodium dodecylsulfate (SDS), diluted with 80 μl of 1 M NaCl, followed by extraction with 25:24:1 phenol/chloroform/isoamyl alcohol (2 x 150 μl). Each sample was then ethanol precipitated after the addition of 25 μg of carrier tRNA. To cleave the apurinic sites, samples were dissolved in 4 μl ddH_2O and 20 μl of an aniline solution (1.2 M aniline, 3.4 M acetic acid). After heating to 40 °C for 30 min, the solutions were diluted with 80 μl 1 M NaCl, then ethanol precipitated. The resultant pellets were redissolved in 80 % formamide and the products were separated by electrophoresis. Gels were visualized either by room temperature exposure to a phosphorimager plate or exposure to Kodak BioMax film at −78 °C.

Acknowledgements: This work was supported by NIH grant GM44853. We thank Dan Erlanson, Scot Wolfe, and Orlando Schärer for a critical reading of the manuscript, and Andrew MacMillan for helpful discussions.

References

1. Klausner, R.D., Rouault, T.A. & Harford, J.B. (1993). Regulating the fate of mRNA: the control of cellular iron metabolism. *Cell* **72**, 19–28.
2. Gait, M.J. & Karn, J. (1993). RNA recognition by the human immunodeficiency virus Tat and Rev proteins. *Trends Biochem. Sci.* **18**, 255–259.
3. Endo, Y., Glück, A. & Wool, I.G. (1991). Ribosomal RNA identity elements for ricin A-chain recognition and catalysis. *J. Mol. Biol.* **221**, 193–207.
4. Szweykowska-Kulinska, Z. & Beier, H. (1992). Sequence and structure requirements for the biosynthesis of pseudouridine in plant pre-$tRNA^{Tyr}$. *EMBO J.* **11**, 1907–1912.
5. Kealey, J.T., Gu, X. & Santi, D.V. (1994). Enzymatic mechanism of tRNA (m^5U54)methyltransferase. *Biochimie* **76**, 1133–1142.
6. Bass, B.L. & Weintraub, H. (1988). An unwinding activity that covalently modifies its double-stranded RNA substrate. *Cell* **55**, 1089–1098.
7. Bass, B.L. & Cech, T.R. (1984). Specific interaction between the self-splicing RNA of *Tetrahymena* and its guanosine substrate: implications for biological catalysis by RNA. *Nature* **308**, 820–826.
8. Guerrier-Takada, C., Gardiner, K., Marsh, T., Pace, N. & Altman, S. (1983). The RNA moiety of ribonuclease P is the catalytic subunit of the enzyme. *Cell* **35**, 849–857.
9. Forster, A.C. & Symons, R.H. (1987). Self-cleavage of plus and minus RNAs of a virusoid and a structural model for the active sites. *Cell* **49**, 211–220.
10. Noller, H.F., Hoffarth, V. & Zimniak, L. (1992). Unusual resistance of peptidyl transferase to protein extraction procedures. *Science* **256**, 1416–1419.
11. Tuerk, C. & Gold, L. (1990). Systematic evolution of ligands by exponential enrichment: RNA ligands to bacteriophage T4 DNA polymerase. *Science* **249**, 505–510.
12. Ellington, A.D. & Szostak, J.W. (1990). *In vitro* selection of RNA molecules that bind specific ligands. *Nature* **346**, 818–822.
13. Sassanfar, M. & Szostak, J.W. (1993). An RNA motif that binds ATP. *Nature* **364**, 550–553.
14. Lorsch, J.R. & Szostak, J.W. (1994). *In vitro* selection of RNA aptamers specific for cyanocobalamin. *Biochemistry* **33**, 973–982.
15. Nieuwlandt, D., Wecker, M. & Gold, L. (1995). *In vitro* selection of RNA ligands to substance P. *Biochemistry* **34**, 5651–5659.
16. Ringquist, S., Jones, T., Snyder, E.E., Gibson, T., Boni, I. & Gold, L. (1995). High-affinity RNA ligands to *Escherichia coli* ribosomes and ribosomal protein S1: comparison of natural and unnatural binding sites. *Biochemistry* **34**, 3640–3648.
17. Tuerk, C., MacDougal-Waugh, S., Hertz, G.Z. & Gold, L. (1994). *In vitro* evolution of functional nucleic acids: high-affinity RNA ligands of the HIV-1 Rev protein. In *The Polymerase Chain Reaction.* (Mullis, K.B., Ferre, F. & Gibbs, R.A., eds), pp. 233–243, Birkhauser, Boston.
18. Wilson, C. & Szostak, J.W. (1995). *In vitro* evolution of a self-alkylating ribozyme. *Nature* **374**, 777–782.
19. Illangasekare, M., Sanchez, G., Nickles, T. & Yarus, M. (1995). Aminoacyl-RNA synthesis catalyzed by an RNA. *Science* **267**, 643–647.
20. Dai, X., De Mesmaeker, A. & Joyce, G.F. (1995). Cleavage of an amide bond by a ribozyme. *Science* **267**, 237–240.
21. Lorsch, J.R. & Szostak, J.W. (1994). *In vitro* evolution of new ribozymes with polynucleotide kinase activity. *Nature* **371**, 31–36.
22. Puglisi, J.D., Tan, R., Calnan, B.J., Frankel, A.D. & Williamson, J.R. (1992). Conformation of the TAR RNA–arginine complex by NMR spectroscopy. *Science* **257**, 76–80.
23. Puglisi, J.D., Wyatt, J.R. & Tinoco, I., Jr. (1990). Conformation of an RNA pseudoknot. *J. Mol. Biol.* **214**, 437–453.
24. Varani, G., Cheong, C. & Tinoco, I., Jr. (1991). Structure of an unusually stable RNA hairpin. *Biochemistry* **30**, 3280–3289.
25. Marino, J.P., Gregorian, R.S., Jr, Csankovszki, G. & Crothers, D.M. (1995). Bent helix formation between RNA hairpins with complementary loops. *Science* **268**, 1448–1454.
26. Pley, H.W., Flaherty, K.M. & McKay, D.B. (1994). Three-dimensional structure of a hammerhead ribozyme. *Nature* **372**, 68–74.
27. Scott, W.G., Finch, J.T. & Klug, A. (1995). The crystal structure of an all-RNA hammerhead ribozyme: a proposed mechanism for RNA catalytic cleavage. *Cell* **81**, 991–1002.
28. Nikonowicz, E.P. & Pardi, A. (1992). Three-dimensional heteronuclear NMR studies of RNA. *Nature* **355**, 184–186.
29. Orita, M., Nishikawa, F., Shimayama, T., Taira, K., Endo, Y. & Nishikawa, S. (1993). High-resolution NMR study of a synthetic oligoribonucleotide with a tetranucleotide GAGA loop that is a substrate for the cytotoxic protein, ricin. *Nucleic Acids Res.* **21**, 5670–5678.
30. Fu, D.-J., Benseler, F. & McLaughlin, L.W. (1994). Hammerhead ribozymes containing non-nucleoside linkers are active RNA catalysts. *J. Am. Chem. Soc.* **116**, 4591–4598.
31. Thomson, J.B., Tuschl, T. & Eckstein, F. (1993). Activity of hammerhead ribozymes containing non-nucleotidic linkers. *Nucleic Acids Res.* **21**, 5600–5603.
32. Ma, M.Y.-X., *et al.*, & Barnett, R.W. (1993). Design and synthesis of RNA miniduplexes via a synthetic linker approach. *Biochemistry* **32**, 1751–1758.
33. Wang, J.-F. & Cech, T.R. (1992). Tertiary structure around the guanosine-binding site of the *Tetrahymena* ribozyme. *Science* **256**, 526–529.
34. Richardson, P.L., Gross, M.L., Light-Wahl, K.J., Smith, R.D. & Schepartz, A. (1994). A uniquely modified RNA: introduction of a single RNA cleavage agent into the M1 ribozyme. *Bioorg. Med. Chem. Lett.* **4**, 2133–2138.
35. Sigurdsson, S.T., Tuschl, T. & Eckstein, F. (1995). Probing RNA tertiary structure: interhelical cross-linking of the hammerhead ribozyme. *RNA* **1**, 575–583.
36. MacMillan, A.M., Query, C.C., Allerson, C.R., Chen, S., Verdine, G.L. & Sharp, P.A. (1994). Dynamic association of proteins with the pre-mRNA branch region. *Genes Dev.* **8**, 3008–3020.
37. Ferentz, A.E. & Verdine, G.L. (1991). Disulfide cross-linked oligonucleotides. *J. Am. Chem. Soc.* **113**, 4000–4002.
38. Ferentz, A.E. & Verdine, G.L. (1994). The convertible nucleoside

approach: structural engineering of nucleic acids by disulfide cross-linking. In *Nucleic Acids and Molecular Biology*. (Eckstein, F. & Lilley, D.M.J., eds), Springer–Verlag, New York.
39. Ferentz, A.E., Keating, T.A. & Verdine, G.L. (1993). Synthesis and characterization of disulfide cross-linked oligonucleotides. *J. Am. Chem. Soc.* **115**, 9006–9014.
40. Wolfe, S.A. & Verdine, G.L. (1993). Ratcheting torsional stress in duplex DNA. *J. Am. Chem. Soc.* **115**, 12585–12586.
41. Erlanson, D.A., Chen, L. & Verdine, G.L. (1993). DNA methylation through a locally unpaired intermediate. *J. Am. Chem. Soc.* **115**, 12583–12584.
42. Wolfe, S.A., Ferentz, A.E., Grantcharova, V., Churchill, M.E.A. & Verdine, G.L. (1995). Modifying the helical structure of DNA by design: recruitment of an architecture-specific protein to an enforced DNA bend. *Chemistry & Biology* **2**, 213–221.
43. Glick, G.D. (1991). Synthesis of a conformationally restricted DNA hairpin. *J. Org. Chem.* **56**, 6746–6747.
44. Lipsett, M.N. (1967). The isolation of 4-thiouridylate disulfide from oxidized transfer ribonucleic acid of *Escherichia coli*. *J. Biol. Chem.* **242**, 4067–4071.
45. Goodwin, J.T. & Glick, G.D. (1994). Synthesis of a disulfide-stabilized RNA hairpin. *Tetrahedron Lett.* **35**, 1647–1650.
46. Endo, Y. & Tsurugi, K. (1987). RNA *N*-glycosidase activity of ricin A-chain: mechanism of action of the toxic lectin nicin on eukaryotic ribosomes. *J. Biol. Chem.* **262**, 8128–8130.
47. Olnes, S. & Pihl, A. (1982). Toxic lectins and related proteins. In *The Molecular Action of Toxins and Viruses*. (Cohen, P. & Van Heynigen, S., eds), pp. 52–105, Elsevier, New York.
48. Endo, Y. & Tsurugi, K. (1988). The RNA *N*-glycosidase activity of ricin A-chain: the characteristics of the enzymatic activity of ricin A-chain with ribosomes and rRNA. *J. Biol. Chem.* **263**, 8735–8739.
49. Holmberg, L. & Nygård, O. (1994). Interaction sites of ribosome-bound eukaryotic elongation factor 2 in 18S and 28S rRNA. *Biochemistry* **33**, 15159–15167.
50. Glück, A., Endo, Y. & Wool, I.G. (1992). Ribosomal RNA identity elements for ricin A-chain recognition and catalysis: analysis with tetraloop mutants. *J. Mol. Biol.* **226**, 411–424.
51. Woese, C.R., Winker, S. & Gutell, R.R. (1990). Architecture of ribosomal RNA: constraints on the sequence of 'tetra-loops'. *Proc. Natl. Acad. Sci. USA* **87**, 8467–8471.
52. Heus, H.A. & Pardi, A. (1991). Structural features that give rise to the unusual stability of RNA hairpins containing GNRA loops. *Science* **253**, 191–194.
53. Szewczak, A.A., Moore, P.B., Chan, Y.-L. & Wool, I.G. (1993). The conformation of the sarcin/ricin loop from 28S ribosomal RNA. *Proc. Natl. Acad. Sci. USA* **90**, 9581–9585.
54. Szewczak, A.A. & Moore, P.B. (1995). The sarcin/ricin loop, a modular RNA. *J. Mol. Biol.* **247**, 81–98.
55. Glück, A., Endo, Y. & Wool, I.G. (1994). The ribosomal RNA identity elements for ricin and for α-sarcin: mutations in the putative CG pair that closes a GAGA tetraloop. *Nucleic Acids Res.* **22**, 321–324.
56. Mol, C.D., Arvai, A.S., Slupphaug, G., *et al.*, & Tainer, J.A. (1995). Crystal structure and mutational analysis of human uracil-DNA glycosylase: structural basis for specificity and catalysis. *Cell* **80**, 869–878.
57. Savva, R., McAuley-Hecht, K., Brown, T. & Pearl, L. (1995). The structural basis of specific base-excision repair by uracil-DNA glycosylase. *Nature* **373**, 487–493.
58. Klimasauskas, S., Kumar, S., Roberts, R.J. & Cheng, X. (1994). *Hha*I methyltransferase flips its target base out of the DNA helix. *Cell* **76**, 357–369.
59. Reinisch, K.M., Chen, L., Verdine, G.L. & Lipscomb, W.N. (1995). The crystal structure of *Hae*III methyltransferase covalently complexed to DNA: an extrahelical cytosine and rearranged base pairing. *Cell* **82**, 143–153.
60. MacMillan, A.M. & Verdine, G.L. (1990). Synthesis of functionally tethered oligodeoxynucleotides by the convertible nucleoside approach. *J. Org. Chem.* **55**, 5931–5933.
61. MacMillan, A.M. & Verdine, G.L. (1991). Engineering tethered DNA molecules by the convertible nucleoside approach. *Tetrahedron* **47**, 2603–2616.
62. Turchinskii, M.F., Guskova, L.I., Khazai, I., Budovskii, E.I. & Kochetkov, N.K. (1970). Chemical method of specific degradation of ribonucleic acids with selectively removed bases. *Molekulyarnaya Biol.* **4**, 428–434.
63. Moore, M.J. & Sharp, P.A. (1992). Site-specific modification of pre-mRNA: the 2'-hydroxyl groups at the splice sites. *Science* **256**, 992–997.
64. Engel, J.D. & von Hippel, P.H. (1974). Effects of methylation on the stability of nucleic acid conformations: Studies at the monomer level. *Biochemistry* **13**, 4143–4158.
65. Wu, T., Ogilvie, K.K. & Pon, R.T. (1989). Prevention of chain cleavage in the chemical synthesis of 2'-silylated oligoribonucleotides. *Nucleic Acids Res.* **17**, 3501–3517.

Received: **8 Aug 1995**; revisions requested: **22 Aug 1995**; revisions received: **22 Sep 1995**. Accepted: **26 Sep 1995**.